










# Quantum acoustics of the Jahn-Teller complexes in doped crystals: Configurational relaxation time as indicator of the complex

M. N. Sarychev <sup>1</sup>, I. V. Zhevstovskikh <sup>1,\*</sup>, N. Yu. Ofitserova <sup>1</sup>, Yu. V. Korostelin <sup>2</sup>, V. A. Ulanov <sup>3,†</sup>, A. V. Egranov <sup>4,‡</sup>,  
V. T. Surikov <sup>5</sup>, N. S. Averkiev <sup>6,§</sup> and V. V. Gudkov <sup>1,||</sup>

<sup>1</sup>*Ural Federal University, Ekaterinburg, 620002, Russia*

<sup>2</sup>*P.N. Lebedev Physical Institute of Russian Academy of Sciences, Moscow, 119991, Russia*

<sup>3</sup>*E.K. Zavoisky Physical-Technical Institute, FRC Kazan Scientific Center of Russian Academy of Sciences, Kazan, 420029, Russia*

<sup>4</sup>*A.P. Vinogradov Institute of Geochemistry, Siberian Branch of Russian Academy of Sciences, Irkutsk, 664033, Russia*

<sup>5</sup>*Institute of Solid State Chemistry, Ural Branch of Russian Academy of Sciences, Ekaterinburg, 620990, Russia*

<sup>6</sup>*Ioffe Institute, St.-Petersburg, 194021, Russia*



(Received 6 August 2023; accepted 20 May 2024; published 4 June 2024)

Experiments carried out with the use of ultrasonic technique in doped crystals have established three mechanisms of relaxation of the Jahn-Teller subsystem at low temperatures. All of them have a quantum nature. The Debye relaxation function  $f_D = 1/(1 + i\omega\tau)$  is changed due to the temperature-dependent relaxation time  $\tau(T)$  provided the frequency  $\omega$  is fixed. The dependence of  $\tau(T)$  derived in an experiment on dissipation or/and dispersion of an ultrasonic wave makes it possible to obtain the temperature dependence of  $f_D(T)$ . As a consequence of quantum nature of the relaxation mechanisms, the dependence of  $\tau(T)$  at low temperatures is an immanent characteristic of the system of Jahn-Teller complexes in a given matrix. Therefore graphical representations of  $-\text{Im}f_D(T)$  and  $-\text{Im}f_D(T)/T$  can serve as fingerprints of a certain Jahn-Teller complex.

DOI: [10.1103/PhysRevB.109.214104](https://doi.org/10.1103/PhysRevB.109.214104)

## I. INTRODUCTION

The term “Jahn-Teller effect” (JTE) embraces a range of phenomena related to the theorem formulated by Hermann Arthur Jahn and Edward Teller in 1937 [1]. Actually usage of “effect” is not quite correct in this case. “Effect” as a noun (meaning “phenomenon”) should relate to a process taking place in time and should represent a response to a certain impact. Regarding the conventional meaning of the JTE, we deal with the symmetry properties that the object possessed before the external action. However, the object does not change these properties after the external action and they manifest themselves in various experiments.

The theorem asserts that a high-symmetry state of a molecule with the orbital degeneracy is unstable, and a stable state is achieved due to deformation that lowers the symmetry of the molecule. Subsequently, this theorem was also applied to crystals in which the Jahn-Teller (JT) center is embedded in the elementary cell, as well as to dilute crystals with small concentration of intentionally introduced impurities [2].

Starting from 1939, experimental works appeared on manifestation of these symmetry properties. It proved to be

that a number of techniques can be used for this aim. The results of investigation of EPR spectra [3–9], ultrasonic attenuation [10,11], quasistatic magnetic and thermal properties [12,13], and optical absorption or fluorescent spectra [14–17] were published along with their theoretical treatment [18–25] (see also references in reviews [26,27] and bibliographic review [28]). In spite of long historical period, attention to such studies is not weakening [29–33]. Contemporary studies of the JTE take place in a number of fields. A few examples relating to solids: cooperative JTE [34–39], anti-JTE [40], JTE in piezoelectrics [41].

At present, optical and magnetic resonance techniques are considered as the most informative methods of investigation of point defects with orbitally degenerated states. The reason of such a reputation is the quantum nature of the resonance transitions between the energy levels  $E_i$  of the JT complexes and small uncertainty of the energies  $\delta E_i$  with respect to the differences between the excited and ground states  $E_i - E_j$ . The other mentioned methods were not widely used. This should be accepted as surprising, particularly with regard to the physical acoustics technique habitually used in solid state research (see, e.g., Refs. [42–48]). Moreover, quantum phenomena, such as acoustic EPR and acoustic NMR also were studied in an ultrasonic/hypersonic experiments (see, e.g., Refs. [49,50] and references therein) and theoretical prediction of resonance absorption of ultrasound by the JT complexes was done in 1963 [51].

Probably, such an attitude was due to nonresonant relaxation nature of the JTE manifestation that was found in the first experiments [10,11]. The relaxation implies the redistribution of the JT complexes over the lowest energy

\*M.N. Mikheev Institute of Metal Physics, Ural Branch of Russian Academy of Sciences, Ekaterinburg, 620137, Russia.

†Kazan State Power Engineering University, Kazan, 420066, Russia.

‡Irkutsk State University, Irkutsk, 664003, Russia; deceased.

§averkiev.les@mail.ioffe.ru

||v.v.gudkov@urfu.ru

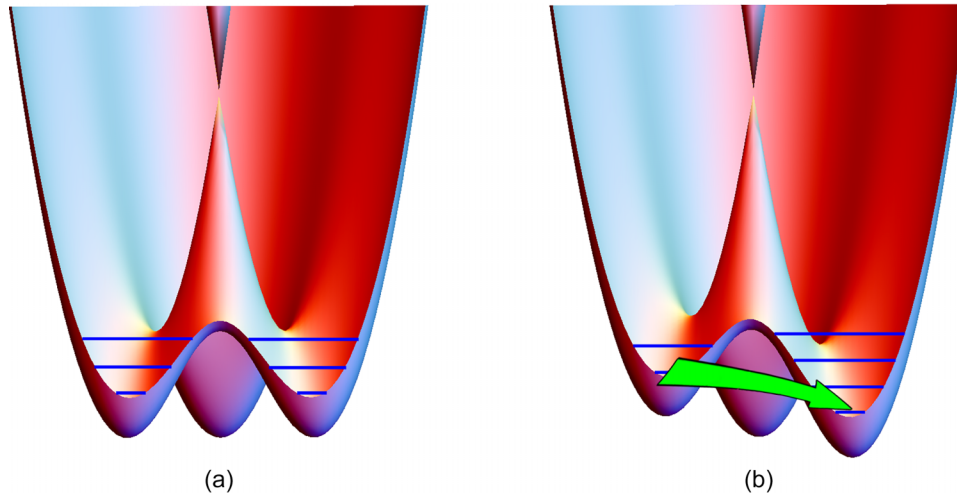


FIG. 1. Three-horn adiabatic potential energy surface of the JT complex subject to the quadratic  $E \otimes e$  problem (a) and its variation caused by an external deformation along a tetragonal coordinate induced by an ultrasonic wave (b). The green arrow shows a tunneling transition to a lower energy state.

ground states modified by the external parameters, e.g., temperature [11] or magnetic field [13]. The status of ignorance of ultrasonic methods remained till 2000s. The tendency to change it was displayed starting with publication of experimental data on manifestation of the JTE in such 3d-doped crystals as  $A^{II}B^{VI}$  (tetrahedral complexes in zinc-blend [52,53] and in wurtzite-type [54] matrices). Later cubal complexes in fluorites [55–57] and tetrahedral complexes in barium hexaferrite with the magnetoplumbite structure [58] were involved in the research orbit of ultrasonics. We should emphasise that the studied relaxation presupposes an establishment of equilibrium over the states corresponding to equivalent JT deformations that carried out an external (mechanical) effect caused by ultrasonic wave propagation. The process is characterized by a macroscopic parameter, i.e., the relaxation time of a distribution function which can be defined as a *configurational (Jahn-Teller or vibronic) relaxation time* stressing its nature and distinguishing it from ones that describe vibrational, spin-spin, or spin-lattice relaxation (see, e.g., Refs. [59,60]).

The question is what parameter (or a number of them) of the JT ensemble as a subsystem of a crystal or of the JT complex itself can be used for its identification in an experiment? Such parameters could be ones entering the vibronic Hamiltonian, namely, the vibronic coupling constants and primary force constants. Combinations of these constants give quantitative characteristics of the adiabatic potential energy surface (APES): the values of global minima and saddle points as well as their positions in symmetrized displacement coordinates. However, the primary force constants should be calculated with the use of optical data and the vibronic coupling constants can be obtained while processing the ultrasonic experimental data only if concentration of the JT complexes is reliably known [61]. The last is actually impossible to realize with the required accuracy if the dopant can form a number of charge states [56].

The configurational relaxation time is the parameter which is free of these disadvantages. Its temperature dependence can be obtained completely in the framework of ultrasonic

experiment regardless of (i) concentration of the dopant, (ii) the polarization of the wave used in the measurements, and (iii) its frequency. In the present paper, we show how the temperature dependence of the configurational relaxation time can be used for the identification of the JT complexes in doped crystals.

## II. METHODOLOGY OF DATA ANALYSIS FOR DETERMINATION OF CONFIGURATIONAL RELAXATION TIME

In the very first publications, the temperature-dependent ultrasonic attenuation  $\alpha_\beta$  was described by Sturge in general terms (Eq. (9.8) in review [26]). In Refs. [10,11], experiments on  $Al_2O_3:Ni^{3+}$  were discussed in which the octahedral complex  $Ni^{3+}O_6$  relates to  $E \otimes e$  JTE problem. It has the APES defined in tetragonal symmetrized coordinates  $Q_\theta, Q_\epsilon$  (in Ham's notation [25]). Such APES is shown in Fig. 1. It has three global minima and three saddle points (see also Ref. [62]). Generalization of this approach to a more complicated APES (namely, defined in the five-dimensional space  $Q_\theta, Q_\epsilon, Q_\xi, Q_\eta, Q_\zeta$ ) and accounting of both dispersion and dissipation lead to the following expression for the JT contribution to the complex wave number of the  $\beta$  normal mode (see, e.g., Eqs. (77) and (78) in Ref. [61]):

$$\frac{k_\beta^{JT}}{k_0} = -\frac{1}{2} \frac{(c_\beta^{JT})^T}{c_0} \frac{1}{1 + i\omega\tau}, \quad (1)$$

where  $k_\beta^{JT} = -k_0(v_\beta^{JT}/v_0) - i\alpha_\beta^{JT}$ ,  $\omega$  is a cyclic frequency,  $\tau$  is the mentioned configurational relaxation time.  $(c_\beta^{JT})^T$  is the isothermal contribution of the JT subsystem to the  $c_\beta$  component of the elastic modulus tensor of a crystal  $\mathbf{c}$ . Phase velocity  $v_0$ ,  $k_0$ , and  $c_0$  are reference magnitudes (the subscript  $\beta$  is omitted for simplicity).  $v_\beta^{JT}$  and  $\alpha_\beta^{JT}$  are contributions of the JT subsystem to the phase velocity and the attenuation of the  $\beta$  normal mode associated with the  $\beta$  component of  $\mathbf{c}$ , respectively. In Eq. (1), the isothermal modulus describes the quasistatic elastic properties of the JT subsystem while the

dynamic properties are determined by the Debye relaxation function  $f_D$ , which can be introduced with the help of real (and positive) functions  $f_1$  and  $f_2$  as

$$f_D = \frac{1}{1 + i\omega\tau} = \frac{1 - i\omega\tau}{1 + (\omega\tau)^2} = f_1 - if_2. \quad (2)$$

The functions  $f_1$  and  $f_2$  depend on the factor of temporal (frequency) dispersion  $\omega\tau$ . If we fix  $\omega$  and change  $\tau$  by means of temperature variation, the low-temperature region will correspond to  $\omega\tau \gg 1$  and oppositely to the high-temperature region  $\omega\tau \ll 1$ . Besides, we introduce  $T = T_1$ , which corresponds to  $\omega\tau = 1$ . Note,  $f_1(T_1) = f_2(T_1)$ .

The explicit form of the isothermal modulus (see, e.g., Ref. [54] for a hexagonal crystal and Ref. [55] for a cubic one) is the following:

$$(c_\beta^{JT})^T = -a_\beta^S \frac{nF_i^2 a_0^2}{k_B T} = -\frac{A_\beta^S}{T}, \quad (3)$$

where  $a_\beta^S$  is a certain (positive) coefficient depending on (i) symmetry properties of the APES global minima, (ii) the crystal symmetry, and (iii) the elastic modulus tensor component  $\beta$ .  $n$  is the concentration of the JT complexes,  $F_i$  is the vibronic coupling constant (tetragonal  $F_E$  or trigonal  $F_T$ ),  $a_0$  is the distance between the JT ion and the nearest neighbor, and  $k_B$  is the Boltzmann constant. So, if to discuss temperature effects, the scale of  $v_\beta^{JT}/v_0$  and  $\alpha_\beta^{JT}/k_0$  variations depend upon  $A_\beta^S/c_0$ , while functional dependencies on  $T$  are governed by  $f_D/T$ .

The  $\tau(T)$  dependence can be retrieved in an ultrasonic experiment, namely, with the use of the data either on attenuation  $\alpha_\beta^{JT}(T)/k_0$  or on phase velocity  $v_\beta^{JT}(T)/v_0$  [61]:

$$\tau(T) = \frac{1}{\omega} \left\{ \frac{\alpha_\beta^{JT}(T_1) T_1}{\alpha_\beta^{JT}(T) T} \pm \sqrt{\left[ \frac{\alpha_\beta^{JT}(T_1) T_1}{\alpha_\beta^{JT}(T) T} \right]^2 - 1} \right\}, \quad (4)$$

$$\tau(T) = \frac{1}{\omega} \sqrt{2 \frac{v_\beta^{JT}(T_1) T_1}{v_\beta^{JT}(T) T} - 1}. \quad (5)$$

the sign “+” is used for  $T < T_1$  and “−” is used for  $T \geq T_1$  due to physical reason: relaxation time is increased with the temperature lowering.

We should emphasize that  $T_1$  enters Eqs. (4) and (5). In the first papers on the JTE (see, e.g., Eq. (14a) in Ref. [11]), the position of the attenuation peak  $T_m$  was used instead being an approximate value of  $T_1$ . The procedure of  $T_1$  determination was also described in detail in Ref. [61]. This adjustment was used in all our papers. It is particularly important if the attenuation peak is observed below 10 K.

### III. UNIVERSAL MECHANISMS OF CONFIGURATIONAL RELAXATION

While discussing the JTE in  $\text{Al}_2\text{O}_3:\text{Ni}^{3+}$  [26], Sturge considered three mechanisms of configurational relaxation: thermal activation, tunneling through the potential energy barriers (analogous to the “direct process” in spin-lattice relaxation), and the two-phonon mechanism (analogous to “Raman” process). The last two mechanisms were analyzed in Ref. [63]. They are accompanied by absorption of one or two phonons, therefore, corresponding relaxation rates are

temperature-dependent. The mentioned three mechanisms (in Sturge notation) are characterized with corresponding relaxation rates, respectively:

$$\tau_a^{-1} = \tau_0^{-1} \exp(-V_0/k_B T), \quad (6)$$

$$\tau_r^{-1} = B T, \quad (7)$$

$$\tau_R^{-1} = (B/\Theta^2) T^3, \quad (8)$$

where  $\tau_0^{-1}$  is the attempts frequency,  $V_0$  is the activation energy,  $B$  and  $\Theta$  are constants. In the discussed by Sturge quadratic  $E \otimes e$  problem,  $B \propto F_E^2/\hbar^4$  and  $B/\Theta^2 \propto F_E^4/\hbar^7$ .

The question was: whether the mentioned mechanisms of relaxation are so universal that they describe relaxation in both cases of linear or quadratic  $T \otimes (e + t_2)$  JTE problem?

The results of our former investigations [56–58,64,65] and initially reported in the present paper (see Figs. 2 and 3 along with Fig. 4 curve 2) give a positive answer to this question at least in the low-temperature region. Certainly, the expressions for  $B$  and  $B/\Theta^2$  (see Ref. [26]) in other than  $E \otimes e$  cases should differ.

The universal form of relaxation mechanisms that we are discussing has been confirmed in one more hexagonal crystal with tetrahedral JT complexes subject to the quadratic  $E \otimes e$  problem ( $\text{BaFe}_{12-x}\text{Ti}_x\text{O}_{19}$  [58]), in the fluorite-structure crystals with cubal JT complexes subject to the quadratic  $T \otimes (e + t_2)$  problem listed in Table I, in  $\text{A}^{\text{II}}\text{B}^{\text{VI}}:\text{Cr}^{2+}$  crystals with tetrahedral JT complexes subject to the linear  $T \otimes (e + t_2)$  problem in sphalerite (Fig. 2) and wurtzite (Fig. 3) matrices.

An analysis of Eq. (1) with account of three mechanisms of relaxation given by Eqs. (6)–(8) in the low-temperature region  $\omega\tau \gg 1$  revealed a linear temperature dependence of velocity and a constant value of attenuation (meaning the JT contribution for both):

$$\frac{v_\beta^{JT}}{v_0} + i \frac{\alpha_\beta^{JT}}{k_0} = \frac{A_\beta^S}{2c_0} \left[ -\frac{B^2 T}{\omega^2} + i \frac{B}{\omega} \right]. \quad (9)$$

The last conclusion (nonzero attenuation at  $T \rightarrow 0$ ) seemed surprising. However, in the first papers, it was believed that the value of  $\alpha_\beta^{JT}(T \rightarrow 0)$  is rather small due to small relaxation rate provided by quantum tunneling process. This belief lasted until the analysis of experimental data of the temperature dependence of attenuation in doped fluorite  $\text{CaF}_2:\text{Cr}^{2+}$  [66].

The conclusion about the finite value of low-temperature attenuation has two consequences: cognitive and practical ones. They are (i) the recognition of a valuable impact of quantum effects in physical acoustics of the JT subsystems at low temperatures and (ii) the necessity to take into account the value of low-temperature attenuation  $\alpha_\beta(T \rightarrow 0)$  while determination of the JT contribution  $\alpha_\beta^{JT}(T)$  to the total attenuation  $\alpha_\beta(T)$ . The last is actually measured in an experiment. The JT contribution to attenuation is a must for constructing the dependence  $\tau(T)$  because it is  $\alpha_\beta^{JT}(T)$  that enters the Eq. (4). Disregard of the finite value of low-temperature attenuation has led to overestimation of the relaxation time magnitude by one or two orders at low temperatures (see, e.g., Fig. 3 in Ref. [55] and Fig. 10 in Ref. [64], Fig. 2(b) (here) and Fig. 4 in Ref. [67], Fig. 3(b) (here) and Fig. 7 in Ref. [54]). However, activation mechanism parameters have been obtained rather

TABLE I. Parameters which characterize configurational relaxation of the JT subsystem in some doped crystals with the fluorite structure. The upper bound of the error is estimated as 5%.

Host crystal	JT ion	$V_0$ , cm $^{-1}$	$\tau_0$ , s	$B$ , s $^{-1}$ K $^{-1}$	$B/\Theta_0^2$ , s $^{-1}$ K $^{-3}$	Ref.
CaF $_2$	Cr $^{2+}$	92	$3.0 \times 10^{-13}$	$5.3 \times 10^6$	$3.2 \times 10^5$	[56]
BaF $_2$	Cu $^{2+}$	94	$2.0 \times 10^{-11}$	$1.4 \times 10^6$	$2.0 \times 10^4$	this paper
CaF $_2$	Cu $^{2+}$	$1.2 \times 10^2$	$3.3 \times 10^{-12}$	$1.5 \times 10^6$	$5.0 \times 10^2$	[57]
SrF $_2$	Cr $^{2+}$	$2.6 \times 10^2$	$7.1 \times 10^{-13}$	$3.6 \times 10^4$	$2.9 \times 10^2$	[65]
CaF $_2$	Ni $^{2+}$	$4.0 \times 10^2$	$1.0 \times 10^{-13}$	$5.6 \times 10^5$	$6.7 \times 10^1$	[64]

accurately due to domination of the activation mechanism at  $T$  nearby  $T_1$  [i.e., in the vicinity of attenuation peak  $\approx \alpha_\beta(T_1)$ , which is larger than  $\alpha_\beta(T \rightarrow 0)$ ].

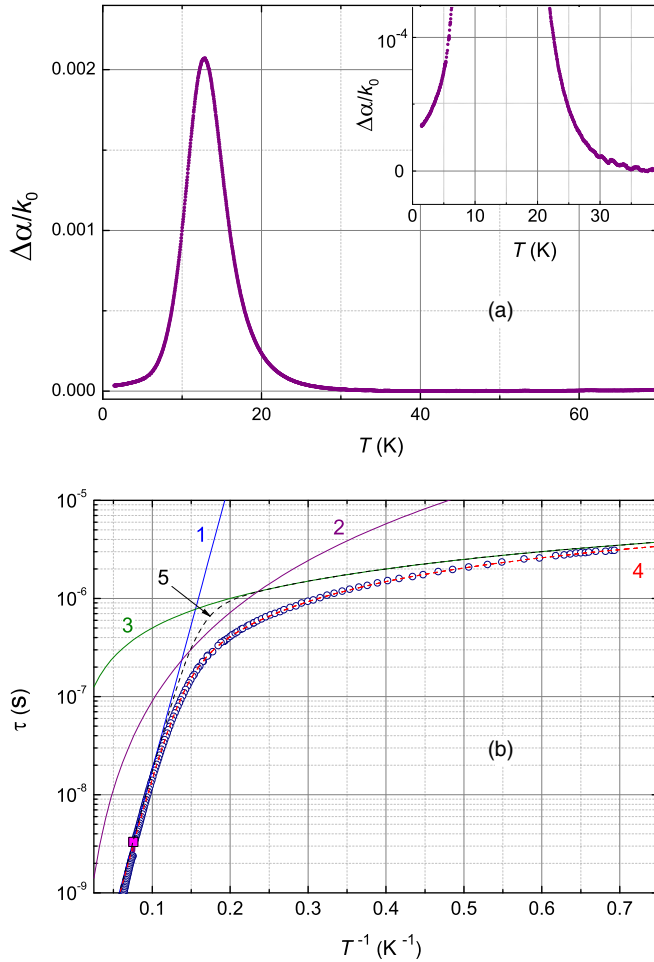


FIG. 2. (a) Temperature dependencies of  $\Delta\alpha/k_0$  for ZnSe:Cr $^{2+}$  obtained at 56.6 MHz.  $\Delta\alpha = \alpha(T) - \alpha(T_0)$ ,  $\Delta v = v(T) - v(T_0)$ ,  $k_0 = k(T_0)$ , and  $T_0 = 50$  K. Transverse normal mode propagating along [110] crystallographic axis with polarization parallel to  $[1\bar{1}0]$  associated with the modulus  $c_E = (c_{11} - c_{12})/2$ . (b) Configurational relaxation time vs inverse temperature (circles) in ZnSe:Cr $^{2+}$ . Model curves  $\tau_a$  (curve 1),  $\tau_R$  (curve 2),  $\tau_t$  (curve 3) are defined by Eqs. (6)–(8). The total relaxation time  $\tau = (\tau_a^{-1} + \tau_t^{-1} + \tau_R^{-1})^{-1}$  (curve 4). Curve 5 shows simulation of relaxation time without account of  $\tau_R$ , i.e.,  $\tau = (\tau_a^{-1} + \tau_t^{-1})^{-1}$ .  $\tau_0 = 2 \times 10^{-11}$  s,  $V_0 = 68$  K = 47.3 cm $^{-1}$ ,  $B^{-1} = 5 \times 10^{-6}$  s K,  $(B/\Theta^2)^{-1} = 9 \times 10^{-5}$  s K $^3$ . The red square symbol corresponds to  $\omega\tau = 1$  at  $\omega/2\pi = 56.6$  MHz.

Determination of the finite value of  $\alpha_\beta^{JT}(T \rightarrow 0)$  can be done with the aid of two independent procedures: (i) simulation of the experimentally obtained a dependence of  $\alpha_\beta(T)$  with the use of the mentioned relaxation mechanisms (like it was done in Ref. [66]) and (ii) construction of the dependencies of  $v_\beta^{JT}(T)/v_0$  with the use of the data obtained on the doped and nominally pure crystals [64], evaluation of configurational relaxation time temperature dependence [using Eq. (5)], and fitting the obtained curve  $\tau(1/T)$  as well with account of the relaxation mechanisms (6)–(8). The fitting procedure can be done with the use of the curve presented in semilogarithmic and linear scales (see Fig. 3). The first variant is useful for exponential  $\tau_a(1/T)$  determination (at high temperatures), the second one helps to define linear  $\tau_t(1/T)$  (low-temperature mechanism). The two-phonon ‘‘Raman’’ mechanism is important in the intermediate range [compare the curves 4 and 5 in Fig. 2(b)].

In ZnSe:Cr $^{2+}$  [Fig. 2(a)], ultrasonic attenuation at  $T > 40$  K approaches to a constant value. We interpret this fact as vanishing the JT contribution to the total attenuation and negligible (with respect to the JT contribution) temperature dependence of the background attenuation at least below 70 K. It makes it possible to assume  $\alpha_\beta^{JT}(T) = \Delta\alpha_\beta(T)$  with  $T_0 = 50$  K.

In CdSe:Cr $^{2+}$  [Fig. 3(a)], high-temperature attenuation does not approach a constant value. It means that additional subsystems (e.g., initiated by excited states, the last are due to high energy barrier  $V_0$ ) can contribute to attenuation. Therefore the procedure of  $\tau(T)$  determination was the following.

(1) Simulation of  $\alpha_{55}^{JT}(T)$  at low temperatures with the use of three mechanisms of relaxation [Eqs. (6)–(8)] and one more fitting parameter given by Eq. (3) was applied for determination of the low-temperature limit of  $\alpha_{55}^{JT}(T \rightarrow 0)$ .

(2) Thereafter, JT contribution was introduced as  $\alpha_{55}^{JT}(T) = \alpha_{55}^{JT}(T \rightarrow 0) + \Delta\alpha_{55}(T)$ , where  $\Delta\alpha_{55}(T) = \alpha_{55}(T) - \alpha_{55}(T = 4 \text{ K})$  is the measured attenuation with respect to its level at  $T = 4$  K.

(3) Evaluation of  $\tau(T)$  [given in Figs. 3(b) and 3(c)] with the use of Eq. (4). This procedure was initially applied for processing the data obtained in doped fluorites and described in Refs. [57,66].

We would like to emphasize that we obtained only the low-temperature dependence of  $\tau(T)$  at stage 1. At stage 3,  $\tau(T)$  was evaluated (using the experimental data) in a more wide temperature range. In this temperature range, accurate consideration requires account for at least part-occupied excited states. As a result we have a number of subsystems with different potential energy barriers (which are lower for the excited states) and, therefore, different values of relaxation time,



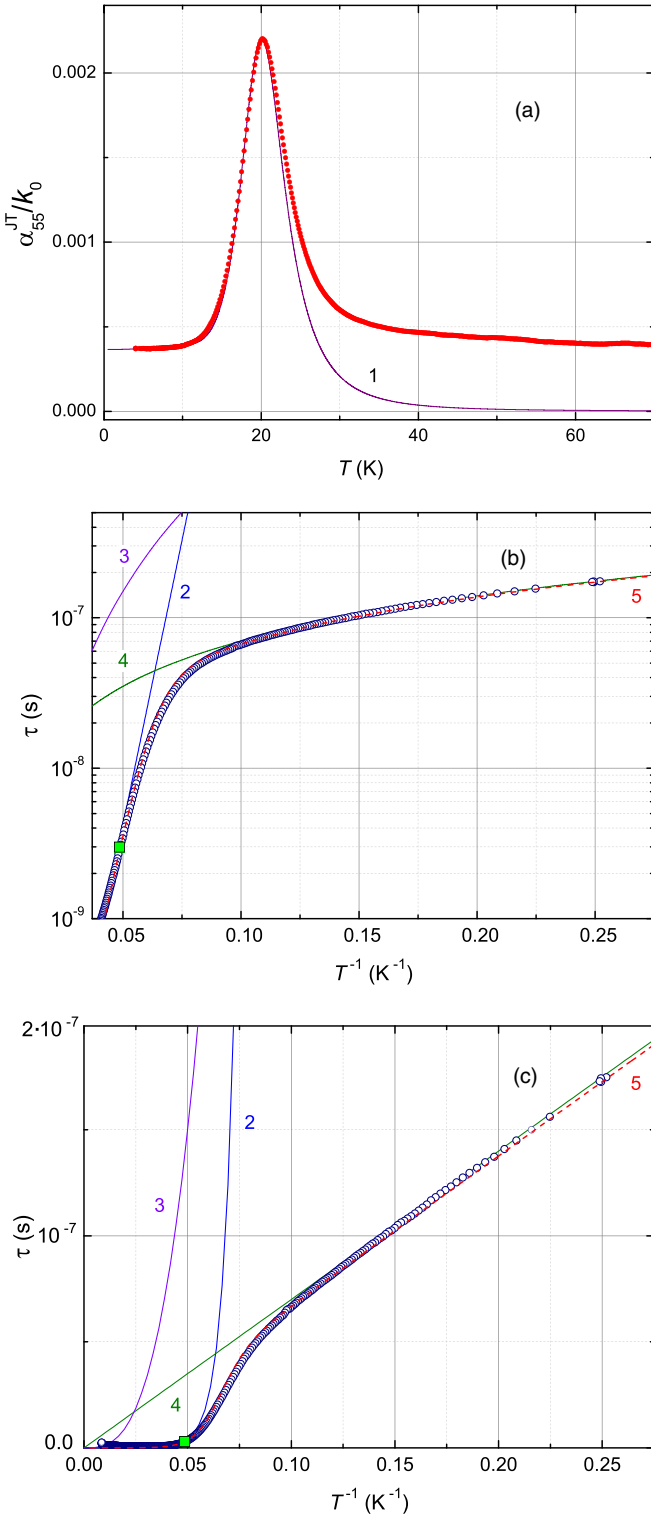


FIG. 3. (a) Temperature dependence of  $\alpha_{55}^{JT}(T)/k_0$  for the  $c_{55}$  mode in CdSe:Cr<sup>2+</sup> (circles) and model curve (1). Configurational relaxation time vs inverse temperature (circles) displayed in semilogarithmic (b) and linear (c) coordinate systems. Model curves  $\tau_a$  (curve 2),  $\tau_R$  (curve 3),  $\tau_i$  (curve 4) are defined by Eqs. (6)–(8). The total relaxation time is shown by curve 5.  $\tau_0 = 0.6 \times 10^{-12}$  s,  $V_0 = 175$  K = 120 cm<sup>-1</sup>,  $B^{-1} = 7.0 \times 10^{-7}$  s K,  $(B/\Theta^2)^{-1} = 1.2 \times 10^{-3}$  s K<sup>3</sup>. The green square symbol corresponds to  $\omega\tau = 1$  at  $\omega/2\pi = 55.3$  MHz.

which contribute to attenuation. So in the case of CdSe:Cr, our consideration of the system as described by one relaxation time is not correct at high temperatures. This is the reason why the experimental curve and the model one differ at  $T > 25$  K.

The number of parameters,  $\tau_0$ ,  $V_0$ ,  $B$ , and  $B/\Theta^2$ , (and  $A_\beta^S$  in the case of CdSe:Cr<sup>2+</sup>) seem to be too many and give a wide field for simulation. However, thermal activation is represented by a linear dependence on the semilogarithmic scale [see Fig. 2(b), curve 1 and Figs. 3(b) and 3(c) curve 2] at high temperatures and it can be processed with the least squares method (actually, meaning measurement not fitting). In CdSe:Cr<sup>2+</sup>, activation energy is 173 K (see description to Fig. 3). It means that the potential energy barrier is high, as a result we have a broad temperature range where the one-phonon mechanism dominates. In this case, the corresponding linear dependence of relaxation time at low temperatures [Fig. 3(c), curve 4] can be also processed with the least squares method (actually, measured as well) and fitting will give the single remaining parameter  $B/\Theta^2$  (and one more,  $A_\beta^S$ , in the case of CdSe:Cr<sup>2+</sup>).

Figures 2(b), 3(b) and 3(c) show that the relaxation time, which characterizes activation mechanism  $\tau_a$ , exceeds  $\tau_i$  and  $\tau_R$  below  $T = 7$  K in ZnSe:Cr<sup>2+</sup> and below  $T = 12$  K in CdSe:Cr<sup>2+</sup> at approximately 55 MHz. Relaxation always is determined by the fastest mechanisms which in the JT subsystems at low temperatures are represented by quantum (tunneling) processes. In view of the variety of the studied types of crystals, we consider this feature as a universal one.

#### IV. UNIVERSAL FORM OF EXPERIMENTAL DATA REPRESENTATION

Ultrasonic investigation of the JTE in doped crystals is based mostly on temperature dependence of contribution of the JT subsystem to attenuation and phase velocity of a normal mode (or to a complex wave number, or to a complex dynamic modulus). The expression for a relative wave number is given by Eq. (1) while the other ones can be obtained with the use of this equation.

The scope of changes of these parameters is determined by  $(c_\beta^{JT})^T/c_0$  [given by Eq. (3)] while the position in a  $T$  scale of their most noticeable variation (peak or smoothed step) is determined by the Debye relaxation function  $f_D$  expressed by Eq. (2) and occurs at  $T = T_m$  which corresponds to  $\omega\tau \approx 1$ . The approximate equality is due to the temperature dependence of the isothermal modulus.

The configurational relaxation time is completely defined by the parameters which describe the quantum-nature processes and activation over the potential energy barrier. Therefore it cannot vary from sample to sample of the same compound. However, it is not convenient to compare the dependencies  $\tau(T)$  obtained in various crystals. We suggest two versions of representation in the form of graphical temperature dependencies for this aim, namely,  $f_2(T)$  and  $f_2(T)/T$ , i.e., the functions which contain the obtained in experiment  $\tau(T)$  but the magnitude of  $\omega$  for calculation of  $f_2$  is chosen by the researcher.

The first one presents the peaks of the same maximum at different positions on the  $T$  scale [ $\max f_2 = f_2(T_1) = 1/2$ ].

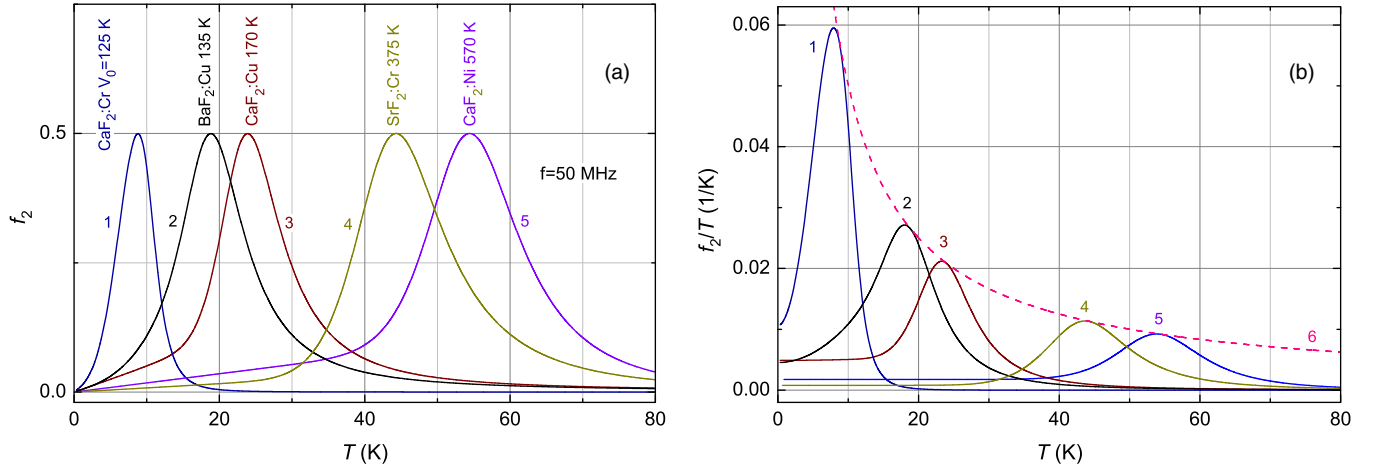


FIG. 4. Variants of graphical representation of the JTE manifestation in an ultrasonic experiment. The fluorite-structure crystals are taken as examples. (a) Temperature dependence of  $f_2$  defined by Eq. (2) as the result of  $\tau(T)$  fitting with account of three mechanisms of relaxation described by Eqs. (6)–(8). (b) Temperature dependence of  $f_2/T \propto \alpha(T)$ . Both were calculated for  $f = \omega/2\pi = 50$  MHz. Curve 6 is the hyperbola  $0.5/T$  on which all the points lay corresponding to  $\omega\tau = 1$ . The parameters which characterize configurational relaxation in these crystals are given in Table I.

Actually, it is determination of  $T_1$  at a given frequency and characterization of the complex by this parameter. The Debye function can be obtained by “normalizing” the measured ultrasonic attenuation  $\Delta\alpha(T)$  to force  $f_2(T_1) = 1/2$ . Such approach is acceptable provided that the value of attenuation at low temperatures is known. In the case of temperature dependence of background attenuation is negligible in the range of the JTE manifestation in an ultrasonic experiment, we can evaluate attenuation with respect to the high-temperature level and assume the measured attenuation as the JT contribution to the total one. In the case of the noticeable temperature dependence of the background attenuation (a conventional situation), it is impossible to use such an approach. Therefore we have to use either (i) simulation of the attenuation curve with the use of three relaxation mechanisms or (ii) the data on ultrasonic velocity (real part of the modulus) and obtain the temperature dependence of the relaxation time with the use of Eq. (5). In both the cases, we construct  $\tau(T)$  and afterwards  $f_2(T)$ .

The experiments are carried out at the frequencies depending on the available piezoelectric transducers. As usual, the fundamental resonant frequency is used (in the range of 10–50 MHz) but sometimes the transducers are excited at the multiple harmonics. Actually we possess the experimental data for each specimen obtained at a certain frequency (or a few number of frequencies). The position of the attenuation peak  $T_m$  on the  $T$  scale is frequency-dependent. So, we have to find the method for presentation of the data at a fixed frequency (chosen by investigator) while initially the data for different crystals were obtained at different frequencies. The proposed method enables to calculate the dependencies for a given  $\omega$  (which actually can be arbitrary as well as corresponding to the frequency related to the experiment on a new specimen for further comparison). The second variant reproduces the form of attenuation curve at a given frequency:

$$\frac{f_2(T)}{T} = \frac{2c_0 \alpha_\beta^{JT}(T)}{A_\beta^S k_0}. \quad (10)$$

Both the forms of the data presentation do not depend neither on concentration of the dopant nor on the polarization and frequency of the wave used in an experiment; the requirements are (i)  $(c_\beta^{JT})^T \neq 0$  meaning  $\alpha_\beta^S \neq 0$  in Eq. (3) and  $f_2$  should be calculated with the use of one chosen frequency.

The example of this approach is shown in Fig. 4 related to the doped fluorite-structure crystals. The magnitudes of the activation energy  $V_0$  are given along with the type of a crystal in Fig. 4(a). At temperatures which are higher than the region of tunneling mechanism domination, activation relaxation prevails since  $\tau_a^{-1} > \tau_t^{-1}, \tau_R^{-1}$ . Exponential  $\tau_a(T)$  dependence leads to fast variation of configurational relaxation time and while passing the point  $\omega\tau = 1$  to construction of the peak of  $f_2(T)$ . Domination of tunneling relaxation at low temperatures is clearly seen in Fig. 4(b):  $f_2/T$  has finite value at  $T \rightarrow 0$ .

Such type of the curves can be considered as indicators of definite JT complexes in a given matrix because the position of the peak on the  $T$  scale at a fixed  $\omega$  is completely determined by the parameters  $\tau_0$ ,  $V_0$ ,  $B$ , and  $B/\Theta^2$  which are actually the fingerprints of the complex (in our example,  $\text{Me}^{2+}\text{F}_8$ , where Me is 3d metal). Since the discussed transitions occur between the levels of vibronic (electron-vibrational) origin and are initiated by the acoustic wave propagation (in a wide interpretation of the term “acoustic wave” meaning elastic waves in the whole possible range of frequencies), the phenomenon does completely relate to the field of quantum acoustics. We believe that quantitative information about the attempt frequency  $\tau_0^{-1}$ , the activation energy  $V_0$ , and the constants  $B$  and  $B/\Theta^2$  can help theorists to construct the APES (similar to one shown in Fig. 1) even in the case when it is defined in five-dimensional space of symmetrized coordinates after obtaining the explicit forms of the constants  $B$  and  $B/\Theta^2$  like it was done for the  $E \otimes e$  JTE problem.

Figure 4 shows that the position of the peak of  $f_2$  or  $f_2/T$  on the  $T$  scale is determined by the magnitude of activation energy  $V_0$ . So, in a case the experimentalist possesses only the

data on  $\alpha(T)$  measured at the frequency  $\Omega$  in a crystal doped by a JT ion which is not studied yet,  $V_0$  can be estimated on the basis the figure similar to Fig. 4 but constructed for the same matrix with  $f_2$  calculated for  $\omega = \Omega$ . We should emphasize that in this case, the experimentalist does not need to process the data to obtain  $\tau(T)$  dependence with subsequent fitting the curve to derive the parameters which characterize relaxation time.

Actually, the figures similar to introduced by Fig. 4 as example, should be drawn separately for  $\text{CaF}_2:3d$ ,  $\text{CdF}_2:3d$ ,  $\text{SrF}_2:3d$ ,  $\text{BaF}_2:3d$ ,  $\text{ZnSe}:3d$ ,  $\text{ZnTe}:3d$ ,  $\text{CdTe}:3d$ ,  $\text{CdSe}:3d$ , etc., to make it possible to recognize the JT impurity in a specimen using the data of ultrasonic experiments without the chemical analysis of the crystal content. It is a significant work which requires proper efforts and time. We hope it will be done in future.

### V. CONCLUSION

(1) We have undertaken analysis of the results of ultrasonic investigation of a number of crystals which contain the cubal or tetrahedral complexes subject to the quadratic  $E \otimes e$  JTE problem or the  $T \otimes (e + t_2)$  one (in linear and quadratic cases). In all the studied crystals, our experiments proved the existence of relaxation mechanisms revealed in the first papers related to octahedral complex subject to the  $E \otimes e$  JTE problem. All of them have a quantum nature that makes it possible to recognize that such experiments appertain to quantum acoustics. The graphical representation of  $\omega\tau/[1 + (\omega\tau)^2]$  or  $\omega\tau/[1 + (\omega\tau)^2]/T$  versus temperature at fixed  $\omega$  can serve as fingerprints (or relaxation signature) of a certain JT complex in a given matrix.

(2) The representation of the results in the form shown in Fig. 4 is given with the use of Eqs. (2), (6)–(8) and the magnitudes of  $\tau_0$ ,  $V_0$ ,  $B$ , and  $B/\Theta^2$  obtained with the help of either fitting or the least squares method. Actually, it is the analytical form of the representation, which makes it possible to display the curves from  $T = 0$  K for any desired temperature. However, the results can be shown *without* simulation but with the use of the experimental data on  $\tau(T)$  similar to ones introduced by the symbols in Figs. 2(b) and 3(b). In this case, we do not restrict ourselves by the definite mechanisms of relaxation but only have an opportunity of *identification* of the unknown JT complex in a given matrix. Simulation

enables quantification of analytical results, i.e., it makes it possible *to retrieve the magnitudes of the parameters* which characterize the mechanisms of relaxation (provided they are verified). Such quantification is a must for further comparison of different JT complexes. The last relates to very crucial issues.

(3) Tunneling transitions between the energy levels located in different minima of the APES can be observed not only in the JT complexes but in any system which possess a simply connected (1-connected) potential energy surface with the minima depending on the orientation or mechanical deformations. In essence, the ultrasonic investigation of all such systems should be referred to quantum acoustics despite the fact that the transitions have a relaxation origin but not a resonant one.

### ACKNOWLEDGMENTS

We acknowledge the support from the Ministry of Science and Higher Education of the Russian Federation (basic part of the government mandate, Project No. FEUZ-2023-0013).

### APPENDIX: EXPERIMENTAL DETAILS

Temperature dependencies of the ultrasonic attenuation and phase velocity were measured with the use of frequency-variable bridge [58,68],  $\text{LiNbO}_3$  piezoelectric transducers, and refrigerator Janis SHI-4H-5 at the Ural Federal University. The relative errors in the measurement of the ultrasonic attenuation and velocity were 0.1 dB and  $10^{-5}$ , respectively.

$\text{ZnSe:Cr}^{2+}$  (concentration of the dopant  $n_{\text{Cr}} = 1.4 \times 10^{18} \text{ cm}^{-3}$ ) and  $\text{CdSe:Cr}^{2+}$  ( $n_{\text{Cr}} = 1.4 \times 10^{19} \text{ cm}^{-3}$ ) were grown by a vapor phase contact-free technique [69] at the P.N. Lebedev Physical Institute.  $\text{SrF}_2:\text{Cr}$  ( $n_{\text{Cr}} = 1.6 \times 10^{19} \text{ cm}^{-3}$ ),  $\text{BaF}_2:\text{Cu}$  ( $n_{\text{Cu}} = 2.9 \times 10^{19} \text{ cm}^{-3}$ ),  $\text{CaF}_2:\text{Cu}$  ( $n_{\text{Cu}} = 7.1 \times 10^{19} \text{ cm}^{-3}$ ), and  $\text{CaF}_2:\text{Cr}$  ( $n_{\text{Cr}} = 4.7 \times 10^{19} \text{ cm}^{-3}$ ) were produced at the E.K. Zavoisky Physical-Technical Institute by the Czochralski method in a helium atmosphere [70].  $\text{CaF}_2:\text{Ni}$  ( $n_{\text{Ni}} = 1.4 \times 10^{19} \text{ cm}^{-3}$ ) were grown from the melt by the Bridgman-Stockbarger method at the A.P. Vinogradov Institute of Geochemistry (see description of the procedure in Ref. [55]). Concentrations of the dopants were determined at the Institute of Solid State Chemistry using an ELAN 9000 ICP-MS quadruple-based instrument (Perkin-Elmer SCIEX).

- 
- [1] H. A. Jahn and E. Teller, Stability of polyatomic molecules in degenerate electronic states - I-orbital degeneracy, *Proc. R. Soc. A* **161**, 220 (1937).
  - [2] J. H. Van Vleck, On the magnetic behavior of vanadium, titanium and chrome alum, *J. Chem. Phys.* **7**, 61 (1939).
  - [3] J. Becquerel and W. Opechowski, Pouvoir rotatoire paramagnétique et aimantation du fluosilicate de nickel hexahydrate, dans la direction de l'axe optique. Le champ cristallin, *Physica* **6**, 1039 (1939).
  - [4] B. Bleaney and D. J. E. Ingram, Paramagnetic resonance in copper fluosilicate, *Proc. Phys. Soc. A* **63**, 408 (1950).
  - [5] R. P. Penrose and K. W. H. Stevens, The paramagnetic resonance from nickel fluosilicate, *Proc. Phys. Soc. A* **63**, 29 (1950).
  - [6] R. E. Coffman, On existence of a third type of Jahn-Teller EPR spectrum in octahedrally coordinated  $\text{Cu}^{++}$ , *Phys. Lett.* **19**, 475 (1965).
  - [7] R. E. Coffman, Paramagnetic resonances of  $\text{Cu}^{++}:\text{MgO}$  at 1.2 K, *Phys. Lett.* **21**, 381 (1966).
  - [8] T. L. Estle and W. C. Holton, Electron-Paramagnetic-Resonance investigation of the superhyperfine structure of iron-group impurities in II-VI compounds, *Phys. Rev.* **150**, 159 (1966).
  - [9] J. T. Vallin and G. D. Watkins, EPR of  $\text{Cr}^{2+}$  in II-VI lattices, *Phys. Rev. B* **9**, 2051 (1974).

- [10] E. M. Gyorgy, M. D. Sturge, D. B. Fraser, and R. C. LeCraw, Observation of Jahn-Teller tunneling by acoustic loss, *Phys. Rev. Lett.* **15**, 19 (1965).
- [11] M. D. Sturge, J. T. Krause, E. M. Gyorgy, R. C. LeCraw, and F. R. Merritt, Acoustic behavior of the Jahn-Teller ion  $\text{Ni}^{3+}$  in  $\text{Al}_2\text{O}_3$ , *Phys. Rev.* **155**, 218 (1967).
- [12] W. Mac, N. T. Khoi, A. Twardowski, J. A. Gaj, and M. Demianiuk, Ferromagnetic  $p-d$  exchange in  $\text{Zn}_{1-x}\text{Cr}_x\text{Se}$  diluted magnetic semiconductor, *Phys. Rev. Lett.* **71**, 2327 (1993).
- [13] W. Mac, A. Twardowski, P. J. T. Eggenkamp, H. J. M. Swagten, Y. Shapira, and M. Demianiuk, Magnetic properties of Cr-based diluted magnetic semiconductors, *Phys. Rev. B* **50**, 14144 (1994).
- [14] R. Pappalardo, D. L. Wood, and R. C. J. Linares, Optical absorption spectra of Ni-doped oxide systems. I, *J. Chem. Phys.* **35**, 1460 (1961).
- [15] M. D. Sturge, Optical spectrum of divalent vanadium in octahedral coordination, *Phys. Rev.* **130**, 639 (1963).
- [16] M. D. Sturge, Jahn-Teller effect in the  ${}^4\text{T}_{2g}$  excited state of  $\text{V}^{2+}$  in  $\text{MgO}$ , *Phys. Rev.* **140**, A880 (1965).
- [17] J. T. Vallin, G. A. Slack, and S. Roberts, Infrared absorption in some II-VI compounds with Cr, *Phys. Rev. B* **2**, 4313 (1970).
- [18] A. Abragam and M. H. L. Pryce, Theoretical interpretation of copper fluorosilicate spectrum, *Proc. Phys. Soc. A* **63**, 409 (1950).
- [19] B. Bleaney and K. D. Bowers, The cupric ion in trigonal crystalline electric field, *Proc. Phys. Soc. A* **65**, 667 (1952).
- [20] H. C. Longuet-Higgins, U. Opik, M. H. L. Pryce, and R. A. Sack, Studies of the Jahn-Teller effect. 2. The dynamical problem, *Proc. R. Soc. A* **244**, 1 (1958).
- [21] U. Opik and H. L. Pryce, Studies of the Jahn-Teller Effect. 1. A survey of the static problem, *Proc. R. Soc. London A* **238**, 425 (1957).
- [22] W. Moffitt and A. D. Liehr, Configurational instability of degenerate electronic states, *Phys. Rev.* **106**, 1195 (1957).
- [23] W. Moffitt and W. Thorson, Vibronic states of octahedral complexes, *Phys. Rev.* **108**, 1251 (1957).
- [24] F. S. Ham, Dynamical Jahn-Teller effect in paramagnetic resonance spectra: orbital reduction factors and partial quenching of spin-orbit interaction, *Phys. Rev.* **138**, A1727 (1965).
- [25] F. S. Ham, Effect of linear Jahn-Teller coupling on paramagnetic resonance in a  ${}^2\text{E}$  state, *Phys. Rev.* **166**, 307 (1968).
- [26] M. D. Sturge, The Jahn-Teller effect in solids, in *Solid State Physics*, Vol. 20, edited by F. Seitz, D. Turnbull, and H. Ehrenreich (Academic Press, 1967), pp. 91–211.
- [27] R. Englman, *The Jahn-Teller Effect in Molecules and Crystals* (Wiley-Interscience, 1972).
- [28] I. B. Bersuker, *The Jahn-Teller Effect, a bibliographic review* (IFI/Plenum, 1984).
- [29] L. Prodan, S. Yasin, A. Jesche, J. Deisenhofere, H.-A. Krug von Nidda, F. Mayr, S. Zherlitsyn, J. Wosnitza, A. Loidl, and V. Tsurkan, Unusual field-induced spin reorientation in  $\text{FeCr}_2\text{S}_4$ : Field tuning of the Jahn-Teller state, *Phys. Rev. B* **104**, L020410 (2021).
- [30] S. V. Streltsov and D. I. Khomskii, Jahn-Teller effect and spin-orbit coupling: friends or foes, *Phys. Rev. X* **10**, 031043 (2020).
- [31] S. V. Streltsov, F. V. Temnikov, K. I. Kugel, and D. I. Khomskii, Interplay of the Jahn-Teller effect and spin-orbit coupling: The case of trigonal vibrations, *Phys. Rev. B* **105**, 205142 (2022).
- [32] N. Iwahara and L. F. Chibotaru, Vibronic order and emergent magnetism in cubic  $d^1$  double perovskites, *Phys. Rev. B* **107**, L220404 (2023).
- [33] P. A. Schultz, A. H. Edwards, R. M. Van Ginhoven, H. P. Hjalmarson, and A. M. Mounce, Theory of magnetic  $3d$  transition metal dopants in gallium nitride, *Phys. Rev. B* **107**, 205202 (2023).
- [34] K. Ji, Z. Wu, X. Shen, J. Wang, and J. Zhang, Jahn-Teller distortion driven ferromagnetism in perovskite monolayer, *Phys. Rev. B* **107**, 134431 (2023).
- [35] V. Kocsis, Y. Tokunaga, T. R  m, U. Nagel, J. Fujioka, Y. Taguchi, Y. Tokura, and S. Bord  cs, Spin-lattice and magneto-electric couplings enhanced by orbital degrees of freedom in polar multiferroic semiconductors, *Phys. Rev. Lett.* **130**, 036801 (2023).
- [36] J. Zhang, Y. Zhou, F. Wang, X. Shen, J. Wang, and X. Lu, Coexistence and coupling of spin-induced ferroelectricity and ferromagnetism in perovskites, *Phys. Rev. Lett.* **129**, 117603 (2022).
- [37] Y. Otsuki, S. Kimurau, S. Awaji, and M. Nakano, Enhancement of the magnetoelectric effect using the dynamic Jahn-Teller effect in a transition-metal complex, *Phys. Rev. Lett.* **128**, 117601 (2022).
- [38] K. Geirhos, J. Langmann, L. Prodan, A. A. Tsirlin, A. Missiul, G. Eickerling, A. Jesche, V. Tsurkan, P. Lunkenheimer, W. Scherer, and I. K  zsm  rki, Cooperative cluster Jahn-Teller effect as a possible route to antiferroelectricity, *Phys. Rev. Lett.* **126**, 187601 (2021).
- [39] Y.-J. Kim, H.-S. Park, and C.-H. Yang, Raman imaging of ferroelastically configurable Jahn-Teller domains in  $\text{LaMnO}_3$ , *npj Quantum Mater.* **6**, 62 (2021).
- [40] N. Feng, J. Han, C. Lin, Z. Ai, C. Lan, K. Bi, Y. Lin, K.-H. Xue, and B. Xu, Anti-Jahn-Teller effect induced ultrafast insulator to metal transition in perovskite  $\text{BaBiO}_3$ , *npj Comput. Mater.* **8**, 226 (2022).
- [41] S. Wang, A. A. Khan, S. Teale, J. Xu, D. H. Parmar, R. Zhao, L. LinGrater, P. Serles, Y. XuZou, T. Filleter, D. S. Seferos, D. Ban, and E. H. Sargent, Large piezoelectric response in a Jahn-teller distorted molecular metal halide, *Nat. Commun.* **14**, 1852 (2023).
- [42] R. Truell, C. Elbaum, and B. B. Chick, *Ultrasonic Methods in Solid State Physics* (Academic Press, New York, 1969).
- [43] J. W. Tucker and V. W. Rampton, *Microwave Ultrasonics in Solid State Physics* (North-Holland Publishing Company, Amsterdam, 1972).
- [44] V. V. Gudkov and J. D. Gavenda, *Magnetoacoustic Polarization Phenomena in Solids* (Springer, Berlin, 2000).
- [45] B. Luthi, *Physical Acoustics in the Solid State* (Springer, Berlin, 2005).
- [46] T. Yamaguchi, Y. Nemoto, T. Goto, M. Akatsu, T. Yanagisawa, O. Suzuki, H. Kitazaw, and T. Komatsubara, Tunneling and rattling of clathrate crystals  $\text{Ce}_3\text{Pd}_{20}\text{Ge}_6$  and  $\text{La}_3\text{Pd}_{20}\text{Ge}_6$ , *Phys. B: Condens. Matter* **359-361**, 296 (2005).
- [47] Q. Baba, T. Goto, Y. Nagai, M. Akatsu, H. Watanabe, K. Mitsumoto, T. Ogawa, Y. Nemoto, and H. Yamada-Kaneta, Quadrupole effects of vacancy orbital in boron-doped silicon, *J. Phys. Soc. Jpn.* **80**, 094601 (2011).
- [48] J. D. N. Cheeke, *Fundamentals and Applications of Ultrasonic Waves* (Taylor & Francis Group, Boca Raton, London, New York, 2012).



- [49] W. G. Proctor and W. H. Tanntila, Saturation of nuclear electric quadrupole energy levels by ultrasonic excitation, *Phys. Rev.* **98**, 1854 (1955).
- [50] A. V. Alekseev and U. K. Kopvillem, Dynamics of ultrasonic propagation in metals with paramagnetic impurities, *Zh. Eksp. Teor. Fiz.* **62**, 1092 (1972) [*Sov. Phys. JETP* **35**, 578 (1972)].
- [51] I. B. Bersuker, Strong resonance absorption of ultrasound in octahedral transition metal complexes involving inversion splitting, *J. Exptl. Theoret. Phys.* **44**, 1577 (1963) [*Sov. Phys. JETP* **17**, 1060 (1963)].
- [52] V. V. Gudkov, A. T. Lonchakov, V. I. Sokolov, and I. V. Zhevstovskikh, Relaxation in ZnSe:Cr<sup>2+</sup> investigated with longitudinal ultrasonic waves, *Phys. Rev. B* **73**, 035213 (2006).
- [53] V. V. Gudkov, A. T. Lonchakov, V. I. Sokolov, I. V. Zhevstovskikh, and V. T. Surikov, Ultrasonic investigation of ZnSe:V<sup>2+</sup> and ZnSe:Mn<sup>2+</sup>: Lattice softening and low-temperature relaxation in crystals with orbitally degenerate states, *Phys. Rev. B* **77**, 155210 (2008).
- [54] N. S. Averkiev, I. B. Bersuker, V. V. Gudkov, I. V. Zhevstovskikh, M. N. Sarychev, S. Zherlitsyn, S. Yasin, Y. V. Korostelin, and V. T. Surikov, Ultrasonic determination of the Jahn–Teller effect parameters in impurity-containing crystals, *J. Exp. Theor. Phys.* **129**, 72 (2019).
- [55] M. N. Sarychev, W. A. L. Hosseny, A. S. Bondarevskaya, I. V. Zhevstovskikh, A. V. Egranov, O. S. Grunskiy, A. T. Surikov, N. S. Averkiev, and V. V. Gudkov, Adiabatic potential energy surface of the Jahn-Teller complexes in CaF<sub>2</sub>:Ni<sup>2+</sup> crystal determined from experiment on ultrasonic attenuation, *J. Alloys Compd.* **848**, 156167 (2020).
- [56] M. N. Sarychev, W. A. L. Hosseny, V. V. Gudkov, I. V. Zhevstovskikh, V. A. Ulanov, G. S. Shakurov, A. V. Egranov, V. T. Surikov, N. S. Averkiev, and V. V. Gudkov, Manifestation of the Jahn–Teller effect subject to quadratic  $T \otimes (e + t_2)$  problem in ultrasonic attenuation. case study of CaF<sub>2</sub>:Cr crystal with isovalent and aliovalent substitution, *J. Phys.: Condens. Matter* **34**, 225401 (2022).
- [57] M. N. Sarychev, W. A. L. Hosseny, I. V. Zhevstovskikh, V. A. Ulanov, A. V. Egranov, A. T. Surikov, N. S. Averkiev, and V. V. Gudkov, Adiabatic potential energy surface of the Jahn-Teller Cu<sup>2+</sup>F<sub>8</sub><sup>−</sup> complexes in a fluorite crystal, *J. Exp. Theor. Phys.* **135**, 473 (2022).
- [58] V. V. Gudkov, M. N. Sarychev, S. Zherlitsyn, I. V. Zhevstovskikh, N. S. Averkiev, D. A. Vinnik, S. A. Gudkova, R. Niewa, M. Dressel, L. N. Alyabyeva, B. P. Gorshunov, and I. B. Bersuker, Sub-lattice of Jahn-Teller centers in hexaferrite crystal, *Sci. Rep.* **10**, 7076 (2020).
- [59] S. R. Rather and G. D. Scholesy, Slow intramolecular vibrational relaxation leads to long-lived excited-state wavepackets, *J. Phys. Chem. A* **120**, 6792 (2016).
- [60] J. Park, Y. Luo, J. J. Zhou, and M. Bernardi, Many-body theory of phonon-induced spin relaxation and decoherence, *Phys. Rev. B* **106**, 174404 (2022).
- [61] V. V. Gudkov, Ultrasonic consequences of the Jahn-Teller effect, in *The Jahn-Teller Effect: Fundamentals and Implications for Physics and Chemistry*, edited by H. Köppel, D. R. Yarkony, and H. Barentzen (Springer, Berlin, Heidelberg, 2009), pp. 743–766.
- [62] I. B. Bersuker, *The Jahn-Teller Effect* (Cambridge University Press, 2006).
- [63] R. Pirc, B. Zeks, and P. Gosar, Kinetics of the alignment of O<sub>2</sub><sup>−</sup> centers in stressed alkali halide crystals, *J. Phys. Chem. Solids* **27**, 1219 (1966).
- [64] M. N. Sarychev, A. S. Bondarevskaya, I. V. Zhevstovskikh, V. A. Ulanov, G. S. Shakurov, A. V. Egranov, V. T. Surikov, N. S. Averkiev, and V. V. Gudkov, Relaxation contribution of a system of Jahn-Teller complexes to the elastic moduli of doped fluorites, *J. Exp. Theor. Phys.* **132**, 790 (2021).
- [65] M. N. Sarychev, W. A. L. Hosseny, A. S. Bondarevskaya, G. S. Shakurov, V. A. Ulanov, V. T. Surikov, I. V. Zhevstovskikh, N. S. Averkiev, and V. V. Gudkov, Adiabatic potential energy surface of the Jahn-Teller complexes in SrF<sub>2</sub>:Cr<sup>2+</sup> crystal, *AIP Conf. Proc.* **2313**, 030071 (2020).
- [66] M. N. Sarychev, A. S. Bondarevskaya, I. V. Zhevstovskikh, A. V. Egranov, O. S. Grunskiy, A. T. Surikov, N. S. Averkiev, and V. V. Gudkov, Tunneling mechanisms of relaxation of the Jahn-Teller complexes in CaF<sub>2</sub>:Cr<sup>2+</sup> crystal, *J. Exp. Theor. Phys. Lett.* **113**, 47 (2021).
- [67] N. S. Averkiev, I. B. Bersuker, V. V. Gudkov, I. V. Zhevstovskikh, K. A. Baryshnikov, M. N. Sarychev, S. Zherlitsyn, S. Yasin, and Y. V. Korostelin, Adiabatic potential energy surface of the Jahn-Teller complexes in CaF<sub>2</sub>:Ni<sup>2+</sup> crystal determined from experiment on ultrasonic attenuation, *Phys. Rev. B* **96**, 094431 (2017).
- [68] N. S. Averkiev, I. B. Bersuker, V. V. Gudkov, I. V. Zhevstovskikh, M. N. Sarychev, S. Zherlitsyn, S. Yasin, G. S. Shakurov, V. A. Ulanov, and V. T. Surikov, The Jahn-Teller effect in elastic moduli of cubic crystals: General theory and application to strontium fluorite doped with chromium ions, in *Fluorite: Structure, Chemistry and Applications*, edited by M. van Asten (Nova Science Publishers, New York, 2019), Chap. 2, pp. 111–160.
- [69] V. A. Akimov, M. P. Frolov, Y. V. Korostelin, V. I. Kozlovsky, A. I. Landman, Y. P. Podmar'kov, and Y. K. Skasyrsky, Vapor growth of CdSe:Cr and CdS:Cr single crystals for mid-infrared lasers, *Opt. Mater.* **31**, 1888 (2009).
- [70] V. A. Ulanov, M. M. Zaripov, E. P. Zheglov, and R. M. Eremina, Trimers of bivalent copper impurity ions in CaF<sub>2</sub> crystals: The structure and mechanism of formation, *Phys. Solid State* **45**, 73 (2003).